Diagenesis of the Upper Bahi Formation in the West of Az Zahrah (B) Field, Az Zahrah - Al Hufrah Platform, NW Sirt Basin, Libya

Muftah Ahmid*

تغيرات ما بعد النشأه المتأخرة التي طرأت على الجزء العلوي من تكوين الباهي غرب حقل الظهرة (ب)، بمسطح الظهرة ـ الحفرة، شمال غرب حوض سرت، ليبيا

مفتاح أحميد

يتكون الجزء العلوي من تكوين الباهي من رمال أركوزية إلى تحت أركوزية ترسبت تحت ظروف بيئية قارية وبحرية تأثرت كثيراً بتغيرات النشأه المتأخرة. خلال مرحلة الترسيب الأولى طرأت بعض التغيرات على ترسبات الرمال النهرية فقد تعرضت لتكون مواد لاحمة مثل الكاولين والبايرايت والهيماتايت. أما ترسبات الرمال البحرية فقد تعرضت لنشاط الكائنات الدقيقة وبداية التضاغط الميكانيكي وترسب مواد لاحمة مثل الكلسايت والدولومايت بالإضافة إلى ترسب معدن الجلوكونايت، بينما ترسب معدن البايرايت في بعض الأماكن.

حدث الذوبان التضاغطي (التضاغط الكيميائي) خلال مرحلة الدفن، ونتج عنه ذوبان معدن السيليكا الذي ساعد في ترسب الكساء الأول لحبيبات الكوارتز وتسبب في انخفاض مؤثر للمسامية الأولية. كان هذا مسبوقاً بترسب كساء حبيبات الفلدسبار والمواد اللاحمة مثل كربونات الكالسيوم التي ساهمت هي الأخرى في إنخفاض مسامية ما بين الحبيبات. بينما تعززت المسامية الداخلية للحبيبات بسبب الذوبان أو الحث الجزئي أو الكلي لحبيبات الفلدسبار وتحولها إلى البايت أو كاولين.

تطورت المسامية الثانوية نتيجة ذوبان المواد اللاحمة مثل كربونات الكالسيوم وغيرها وعلى كل حال، فأن هذه المسامية قد شُغلت جزئياً بالمعادن الطينية مثل الكاولين، ألآيت والكلورايت. وتبُعت هذه التطورات بترسب كساء على حبيبات الكوارتز والتي تظهر من خلال احتوى كساء حبيبات الكوارتز لكساء حبيبات الفلدسبار وللمعادن الطينية المتكونة مبكراً. هذا بالإضافة إلى ترسب مواد لاحمة مثل الدولومايت والدولومايت الحديدي والأنهيدرايت التي تدل علي إنها ترسبت متأخر نسبياً. فقد سبب تراكم سمك الطبقات المترسبة زيادة تأثير التضاغط ونتج عن فعل سوائل الطبقات حث وذوبان المكونات الصخرية التي ساهمت في تحسن المسامية ولكن ترسب مواد لاحمة متأخرة كان له تأثير عكسي.

تظهر هذه الدراسة بأن الحث الناتج عن تغيرات النشأة المتأخرة كان له كبير الأثر على جودة وتقييم صخور المكمن وعلى المكونات الأصلية للرمل.

ABSTRACT: *The Upper Bahi Formation studied samples are arkosic to subarkosic arenites, deposited under continental and marine conditions. The sandstones are strongly affected by diagenesis. During the* **eodiagenesis, stage** *the fluvial sands were subjected to formation of early kaolin, pyrite and heamatite cements, whereas bioturbation, precipitation of calcite and dolomite cements, glauconite and localized pyrite took place in the marine sands.*

Pressure dissolution (chemical compaction) took place during the **mesodiagenesis stage,** *which supplied silica for the precipitation of first quartz over growths, and thus induced a considerable reduction of primary porosity. Cementation by feldspar overgrowth and carbonates contributed to a considerable reduction of the intergranular porosity. Partial to complete dissolution, albtization and kaolinization of feldspar grains also occurred*

* Libyan Petroleum Institute.
E-mail: akhmuftah@yahoo.com

and resulted in the enhancement of the intragranular porosity.

Secondary porosity has also been developed by the dissolution of interstitial cements such as carbonates. However, this porosity is partially occluded by clay minerals such as kaolin, illite, and chlorite.

These processes were followed by precipitation of quartz overgrowth that engulfed feldspar overgrowths and authigenic clay minerals, as well as local development of non-ferroan dolomite and anhydrite cements. Overburden sediments increased the compaction effects, and the action of formation fluids resulted further alteration and dissolution of the framework grains which enhanced the porosity, but precipitation of late cements had a reversed effect.

This study has shown that the diagenetic alteration have had a considerable impact on reservoir quality evaluation and on the original composition of the sandstones.

INTRODUCTION

The Bahi Formation is present in the northweast of the Sirt Basin, in the Az Zahrah – Al Hufrah platform (Fig. 1). The formation had been studied by Baird (1964), Barr and Weegar (1972) Saghair (1990) and Khalifa (1997).

This study aims to identify the diagenetic processes in terms of biological, physical and chemical changes, which had been taken place after sediments deposition and at different burial depths and aims also to evaluate their effect on reservoir quality sediments such as porosity.

Petrographic description, scanning electronic microscopy, backscatter electron imaging, cathodoluminescence, clay minerals separation and X-ray diffraction are the techniques used in evaluating the evidence for diagenesis processes. Sixty polished thin sections were prepared from the cores of the wells: JJ-132, Q1-32, LL1-32, FF1-32, II1-32 and MM1-32, for the study.

DIAGENESIS PROCESSES IN THE UPPER BAHI FORMATION

Three main diagenesis processes were recognized during the study of the available samples, these can be described as follow:

Biological Changes

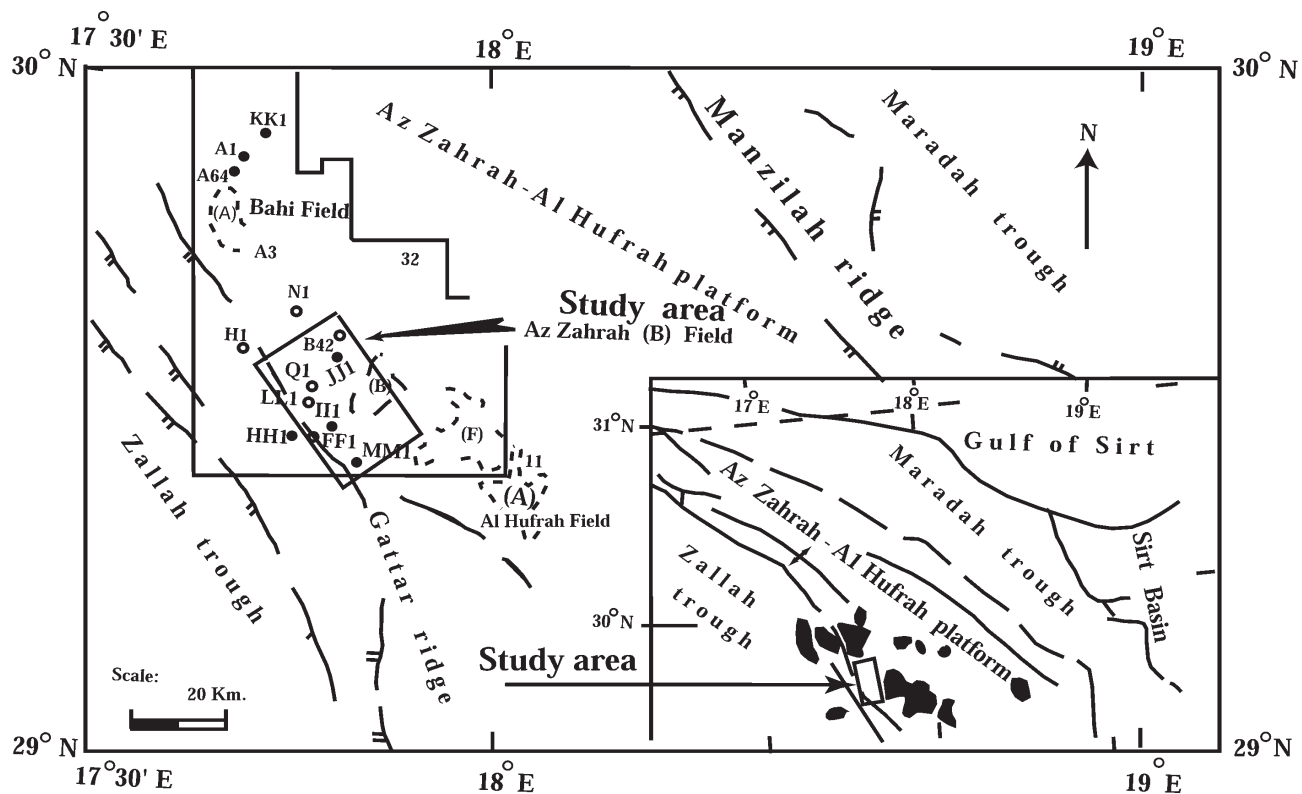The Uppermost Bahi Formation shows traces of

Fig. 1. Location map of the study area *(After Khalifa, 1997).*

bioturbation destroying structure of interbedded mudstone - very fine siltstone lamina in MM 1-32 at depth 4928´ (-3771ft). The sample exhibits micro-scale vertical burrows (Plate I-1), and this may suggest a near-surface shallow water (near shore zone?) depositional environment.

Physical Changes

The Upper Bahi Formation displays examples of several physical changes, including fracturing, deformation and pressure dissolution features, which can be seen in grain morphology and their contact relationships.

Fracturing of grains can be seen in Plate.I-2, which shows a perthite grain split along cleavage by pressure from an irregularly shaped quartz grain. Deformation of grains is clearly displayed by buckling of mica flakes around more equate grains of quartz and feldspar. It is shown by muscovite (Plates. I-3).

Cold stage cathodoluminescence (-190^{0}C) is used to identify the original grain boundaries from possible quartz overgrowth and cements. Some samples show presence of pressure dissolution; coarse sandstone sequences show several types of detrital grain contacts such as straight and tangential, sutured and concave-convex (Plate. I- 4).

Chemical Changes

Precipitates

The studied samples show precipitation of calcite, dolomite and clay mineral intergranular cements, quartz and feldspar overgrowths, as well as minor developments of anhydrite cement. In addition to, idiomorphic authigenic minerals, which are mainly quartz, orthoclase feldspar and pyrite.

Intergranular Cements

Silica – Chalcedony

It is not common, but occurs as radiating fibers and partial spherulitic structures set in a clay-rich matrix as early diagenetic event (Plate. I-5)

Carbonate Cements

Carbonate cements are present locally in patchy areas or in thin, more continuous units in the studied samples. Its presence causes reduction or complete occlusion of porosity, shows both early and late precipitation of authigenic carbonate cement and occasionally displays corrosion of detrital grains such as quartz and feldspar. The carbonates developed in euhedral and rhombohedral crystals, some of which are zoned as a result of growth of dolomite or calcite crystals, at different period of times in pore fluid of different or/changing chemical composition.

Calcite: Some samples shown calcite cement, it ranges from patchy to totally fill in pore space, causing partial to complete reduction of porosities. It displays a poikilotopic texture and anhedral crystals, whereas early calcite cements prevents the detrital grains from alteration or precipitation of overgrowths (Plate. I-6), the later calcite cement can be recognized by the presence of overgrowths on the detrital grains (Plate. II-1).

The source of the primary calcite is almost certainly from entrapped seawater or, in continental sands from soil development. Later calcite is also from pore water, where the calcium may have originated from clays, dissolution of shell material, or from overlying carbonate-rich formations. Another source might be related to release of calcium form plagioclase feldspars as a result of albitization of feldspar grains.

Dolomite: Dolomite occurs as thin lamina and as pore filling in some samples, with different crystals size ranging from exotopic and idiotopic microcrystalline (Plate. II-2), to coarse euhedral rhombs crystals as shown in Plate II-3. Evidence for replacement or dolomitization of precursor calcium carbonate is seen in the preservation of fossil 'shell' material (Plate. II-4).

Ferroan Dolomite: Antigenic dolomite crystals of sand size or even larger, often display zones of iron-poor and iron rich-dolomite (Plate.II-5). These are commonly the result of growth of the dolomite crystals at different periods of time in fluids of varying composition.

Analysis of ferroan dolomite crystal demonstrates that the percentage of iron content increases gradually with crystal growth, resulting in the different zones grading from crystal centre where the analysis indicates pure dolomite, through zones containing minor amounts of iron to zones of high iron content (Table.1).

Table 1. Chemical composition variation within structure of a ferroan dolomite crystal.
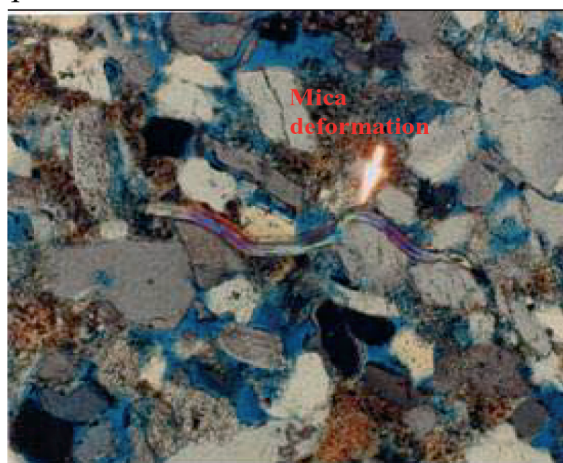
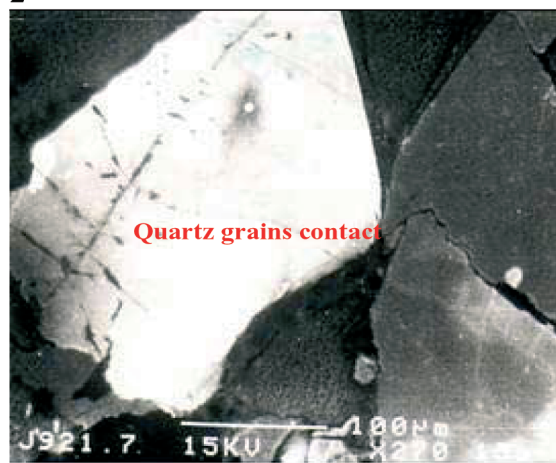| Chemical composition	Dolomite crystal core analysis	Dolomite middle crystal analysis	Dolomite crystal margin analysis
FeO	0.0%	0.83%	8.4%
MgO	18.4%	12.3%	13.5%
CaO	27.3%	26.97%	26.78%
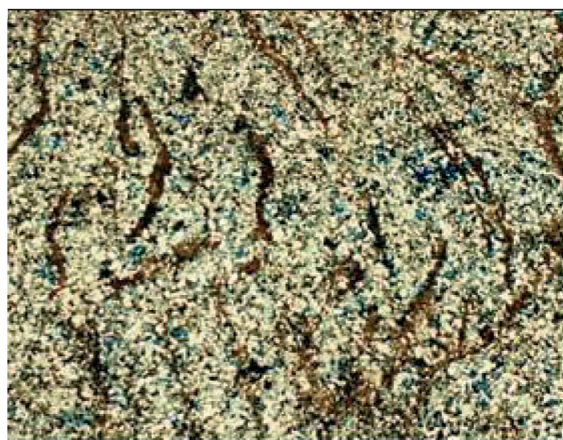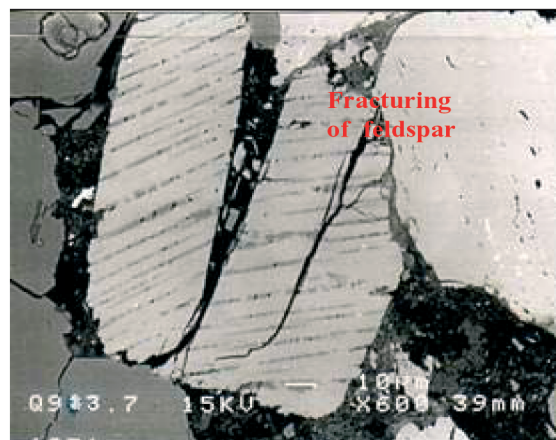
Plate I

Plate I-1   Bioturbation in very fine siltstone /claystone lamina destroying sediments structure. MM1-32, 47282 (-37712 XI2), 32 B.T. XP x2.

Plate I-2   Perthitic potassium feldspar developed along the cleavages. Note open fracture porosity. Q1-32, 49132 (37622), 272 BT. BSE.

Plate I-3   Muscovite flakes bending in between detrital quartz grains due to mechanical compaction. Q1-32, 49132 (-37622), 272 BT. TS. XP x10.

Plate I-4   CL (cold stage −190°C), authigenitic silica cement precipitated on detrital quartz grains. Shows concave-convex grains contact boundaries as a result of compaction and pressure dissolution. JJ1-32, 49212 (-37522) 122 BT.

Plate I-5   Chalcedonic silica cement in radiating form in clay -rich cement. FF1-32, 46512 (-37462), 232 BT. TS. XP. x20.

Plate I-6   Framework grains floating in early poikilotopic calcite cement. Showing corroded margins of quartz grains. JJ1-32, 48242 (37552), 152 BT. TS. XP x5.
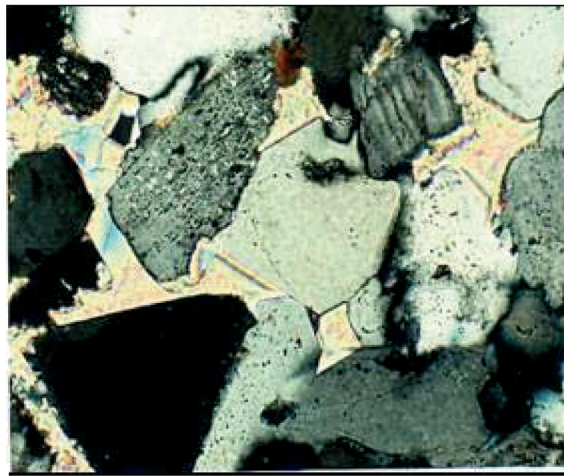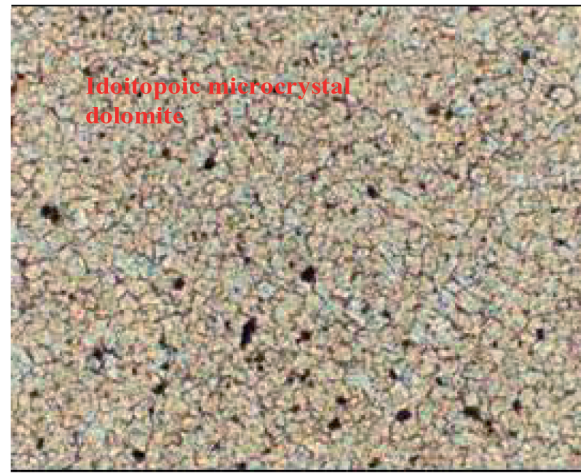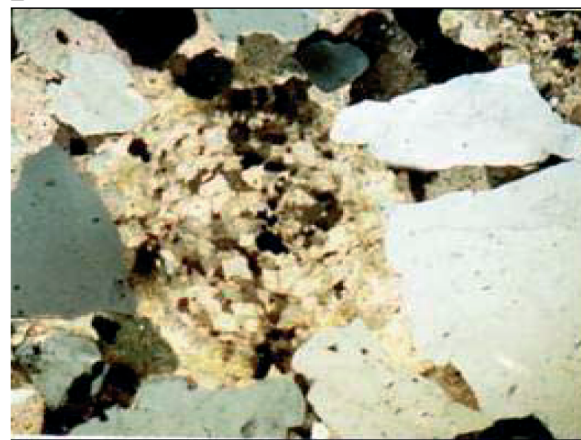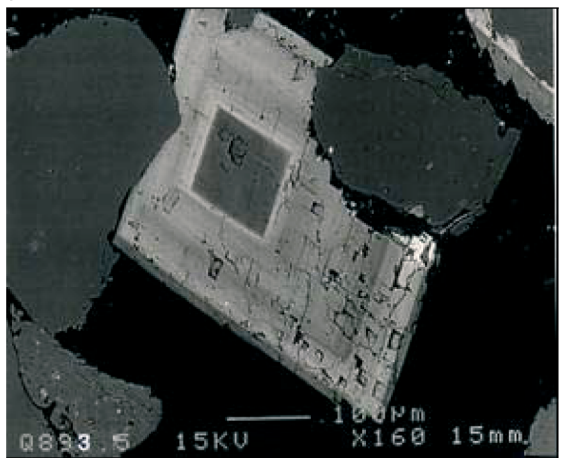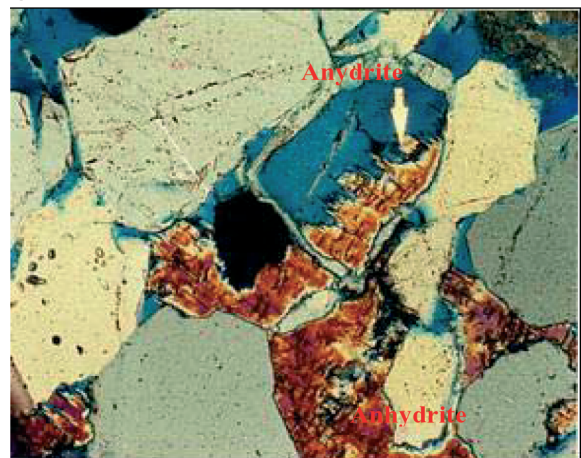
Plate II

Plate II-1   Late poikiotopic calcite cement precipitated after forming quartz overgrowth, shown in straight contact boundaries. II1-32, 48572 (-36962), 82 BT. TS. XP x20.

Plate II-2   Early dense cryptocrystalline dolomite lamina, idiotopic crystals, in mosaic texture associated with scattered microcrystalline authigenic pyrite. LL1-32, 48952 (-37442), 92 BT. TS. XP. x20.

Plate II-3   Early dolomite cement in well developed zoned dolomite crystals. Note replacement of detrital quartz grains margins and absence of silica overgrowth. II1-32, 48962 (36352), 472 BT. TS. XP x20.

Plate II-4   Replacement of unknown microfossil by xenotopic dolomite crystals. II1-32, 48962 (-37352), 472 BT. TS. x10.

Plate II-5   Euhedral zoned ferroan dolomite crystal developed in secondary porosity. Pure dolomite crystal in gray is seen in center. The zoning is due variation in iron content. Q1-32, 48932 (-37422), 72 BT. BSE.

Plate II-6   Late precipitate of poikilotopic authigenitc anhydrite cement in K- feldspar grain porosity, surrounded by overgrowth rims. II1-32, 49012 (37402), 522 BT. TS. XP x10.

Anhydrite

Some samples show local presence of authigenic anhydrite cement, which was precipitated in massive aggregates in intergranular pore space, partially or wholly, surrounded the grains or replacing altered feldspars (Plate. II-6), whereas radiating fibers patterns shown in some samples.

Authigenic Overgrowth

Silica-Quartz: It forms the dominant cement in the upper Bahi Formation. It is mainly silica overgrowth, which occurs on almost all detrital quartz grains with the exception of those, which are enclosed in a well-developed matrix or early carbonate cement.

The quartz overgrowths are commonly beautifully developed and grow in open pore space (Plates. III-1), and can develop at any stage when some porosity is provided. The overgrowths are sometimes picked out by an impurities zone of inclusions of clay or ferruginous material at the host-grain overgrowth contact. Subsequent stages in case of multiple overgrowths can be picked out (Plate. III-2).

Feldspar Overgrowth: It forms the third most important cement in the samples after quartz and carbonate cements. Overgrowth mainly consists of pure potassium feldspar on orthoclase feldspars and pure albite overgrowth on plagioclase (oligoclase and albite).

K-feldspar Overgrowth: K-feldspar grains which display perthitic textures have undergone some changes such as alteration to clay minerals or albitization. Even where the parent grains are relatively unaltered there are commonly some presence of inclusions at the contact between the overgrowth and the host grain. Some overgrowth displays a serrated edge (Plates. III-3).

Plagioclase Feldspar Overgrowth: It is typically albite in composition. It does not display such spectacular overgrowths as K-feldspar at least, the overgrowths are less easy to identify. This may largely be because the parent grains may have been albitized thus losing distinction with the overgrowth.

Minor Authigenic Mineral Precipitates

Pyrite

It is abundant in the studied samples, found scattered throughout the sediments, and partially replaces detrital grains such as feldspar, quartz, dolomite, calcite, phosphatic fragments and mica. It occurs in well developed crystals, in framboidal aggregate form (Plate. III-4) or seen in thin discontinuous lamina filling pore space and minor fissures.

Glauconite

Traces of glauconite are present in few thin sections in the uppermost part of the Bahi Formation, especially in clay-rich lamina, in depths ranges between 20 to 30 feet below the formation top, occasionally in small grains. It is a shallow marine authigenic mineral, early formed from diagenesis of iron rich minerals such as biotite. It is seen in the wells: (FF1-32, II1-32 and Q1-32, Plate. III-5)

Iron Oxides

They are widespread in the Bahi Formation, usually as coatings on the detrital grains or as authigenic cements. Hematite cement is present as traces in the upper part, but dominated in the middle and lower parts, which suggests continental depositional environments (Plate. III-6).

*Dissolution*

Intrastratal Solution

The studied samples display partial to total dissolution of grains. In some, such as with both types of feldspars, thin overgrowth rims and some structure of detrital grains are left behind (Plate. IV-1).

*Alteration*

Alteration of Feldspar

In the upper Bahi Formation authigenic kaolin is observed to be the alteration product of detrital feldspar, occurring as idiomorphic booklets or in vermiform aggregates filling the intergranular / intercrystalline porosity. Albitization or kaolinization of the feldspars is proceed in patches, probably of albite rich areas in the albitized grains (Plate. IV-2). Plagioclase feldspars show that the alteration is proceed along cleavages and fractures planes (Plate. IV-3).
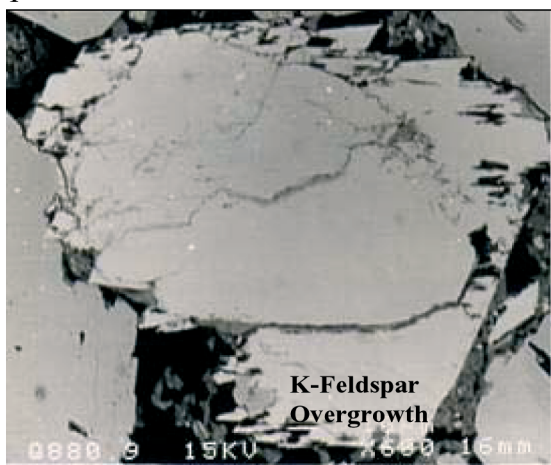
Alteration of Mica

Expanded mica or clay mineral (kaolin) nucleation is present in different forms such as bow tie, alteration of expanded and restricted parts and uniform expanding mica (Plate. IV-4).
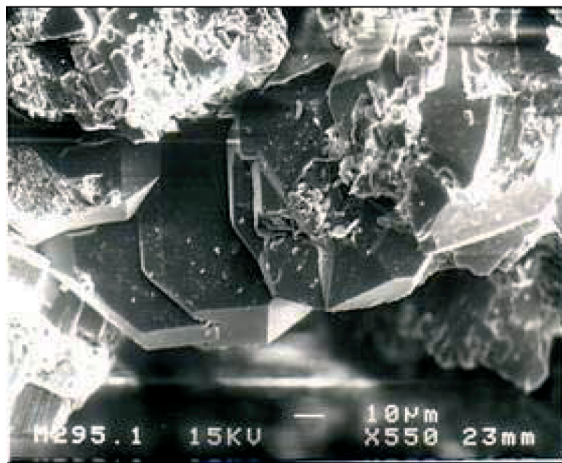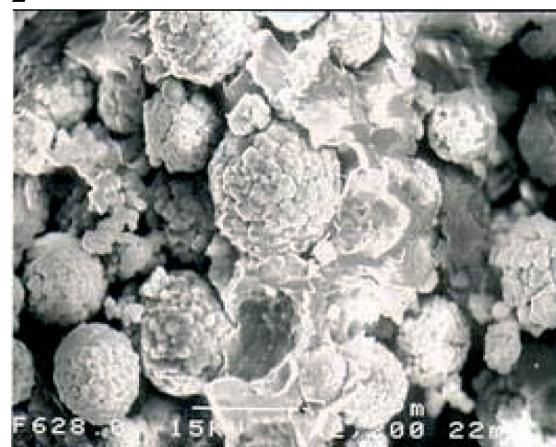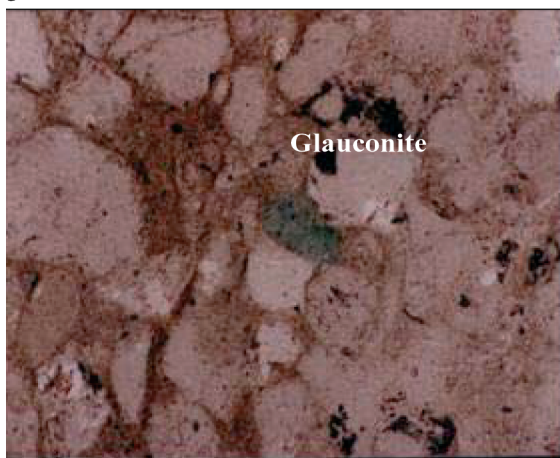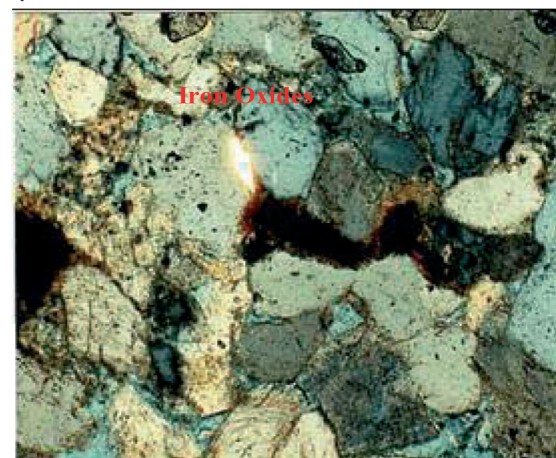
1
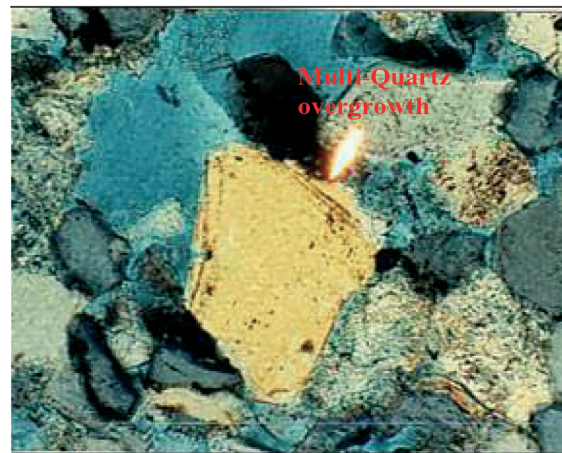
2

3

4

5

6

Plate III

Plate III-1 Well developed quartz overgrowth causing reduction to the intergranular porosity. MM1-32, 4729.52 (-3772.52), 4.52 , BT. SEM.

Plate III-2 Multi-silica overgrowth, distinguished by presence of several inclusion lines. MM1-32, 47482 (-37912), 232 , BT. XP x20.

Plate III-3 Thick k-feldspar overgrowth. Note rhomb shape of adularia crystals and presence of clay inclusion in between the parent grains and overgrowth. Q1-32 48862 (-37372), at FT. BSE.

Plate III-4 Authigenic framboidal pyrite composed of fine aggregates of small and well developed crystals closely packed together. FF1-32 46282 (-37232), at FT. SEM.

Plate III-5 Glauconite grain, an indication for shallow marine depositional environments, the sample represent the uppermost Bahi Formation. Q1-32, 49132, (-37622), 272 BT. TS. XP x20.

Plate III-6 Iron oxides (heamatite) authigenic mineral precipitated as coating or in between detrital grains. MM1-32, 47342 (-37772), 92 BT. TS. XP x 20.
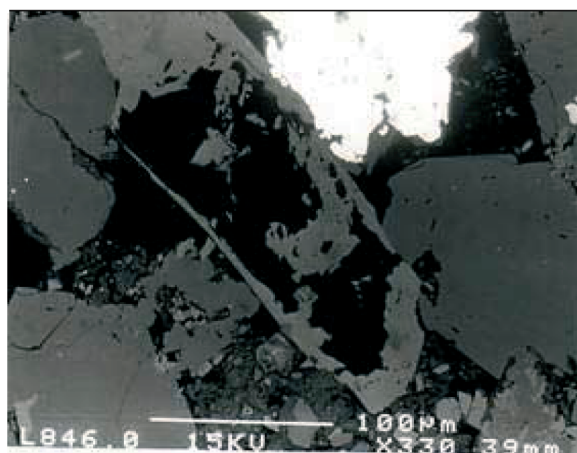
1
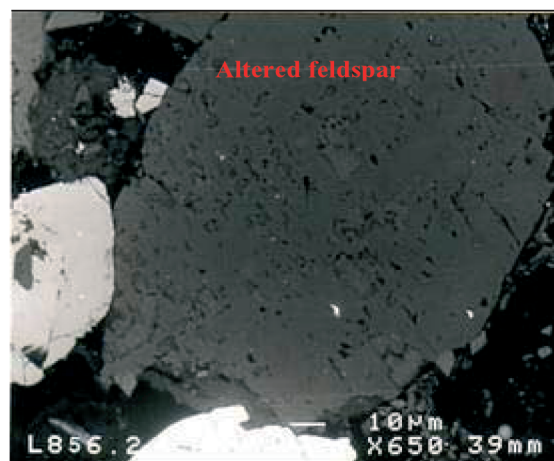
2

3

4

5

6

Plate IV

Plate IV-1   Intragranular porosity developed from almost complete dissolution of detrital plagioclase, leaving behind albite overgrowth rims. LL1-32, 48562 (-37462), 212 BT. BSE.
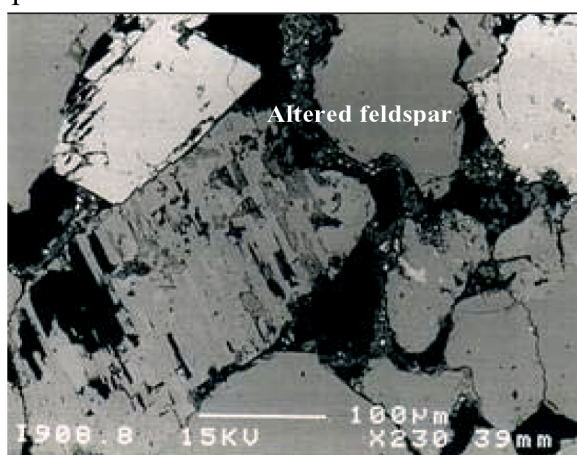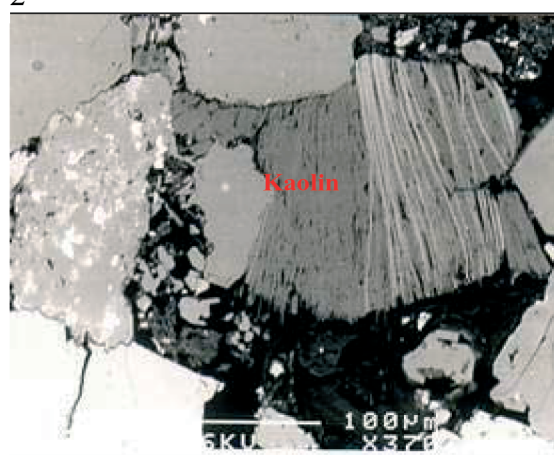
Plate IV-2   Patchy kaolinization and/or albtization of plagioclase feldspar along the grain cleavages. LL1-32, 48562 (-37462), 212 BT. BSE.

Plate IV-3   Plagioclase altered along twin lamellae, displaying albitization and/or kaolinization in some parts and complete dissolution of others developing secondary porosity. II1-32, 49082 (37472), 592 BT. BSE.

Plate IV-4   Uniform expanded mica (white), kaolin (gray), Note that precipitation of quartz overgrowth was earlier than forming kaolin. FF1-32, 46282 (-37232), at FT. BSE.

Plate IV-5   Kaolin crystal booklets inhibiting development of silica overgrowth or quartz overgrowth engulfing authigenic kaolin II1-32, 49082 (37472), 592 BT. BSE.

Plate IV-6   Late authigenic kaolin probably developed from alteration of K-feldspar grains, and preserved within k-feldspar overgrowth rims. LL1-32, 48562 (-37462), 212 BT. TS x20.

Clay Minerals

Clays are well recognized with the common petrogrphical techniques, such as optical microscope, SEM, BSEI and XRD. Illustrate in the plates and (Fig. 2).

Kaolin: It is common in the Bahi Formation where it is easy to distinguish under the microscope and by SEM and BSC by its morphology of euhedral hexagonal crystals and by XRD with heating treatment. At 350^{0}C there is only a slight decrease in the koalin peaks, which then completely collapse at 550^{0}C (Fig. 2). XRD analysis of kaolin is characterized by intensity of first and second order basal reflection at: 7.1Å and 3.5Å, Wilson (1987).

Early kaolin formed before precipitation of quartz overgrowths, in some samples shown engulfing by the quartz overgrowth as in plate (IV-5), whereas the later or authigenic kaolin formed after development of feldspar overgrowth and alteration of detrital feldspar grains (Plate. IV-6).

Illite or Hydromica: This type is one of most common authigenic clay minerals and is distinguished by its hair-like morphology as shown by SEM (Plate. V-1) and proved on XRD analysis (Fig. 2).

Chlorite: Only traces of chlorite were observed by BSC and XRD in several samples.

Albitization of Feldspars

Use of back-scattered technique in analysis of feldspar grains lead to observation of a quasi-perthitic texture, in which potassic and sodic feldspars
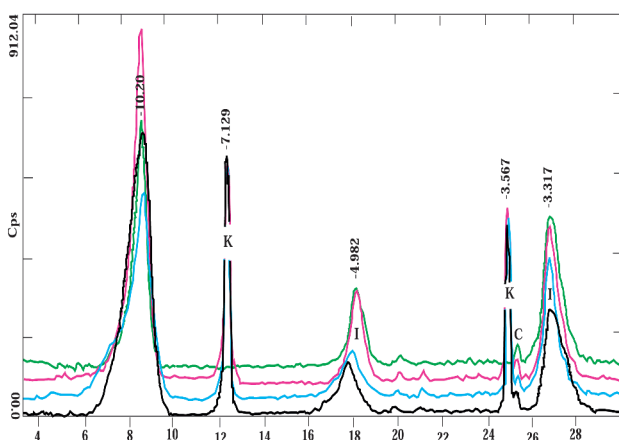

Fig. 2. XRD diffraction patterns of MM1-32, depth 47482 , 232 below formation top. Displays Illite (I) and kaolinite (K), and traces of chlorite (C). The samples temperature patterns are: black: air dried, blue: glycolation, pink: heating to 350^{0}C and green heating to 550^{0}C. *(From Ahmid, 2003).*

are inter-grown in irregular patches or in elongated zones parallel to cleavages; these relationships have been attributed to albitization as noted by Kastner and Siever (1979); Walker (1984) and Saigal *et al.*, (1988). The albitization criteria are: overgrowths purity, lack of inclusions and luminescence, and absence of albitization in presence of early carbonate cement. These were fully noted in the altered feldspar grains, which support the presence of albitization.

In plagioclase grains the albitic areas comprise the same high *purity* albite as overgrowths on the same grain shown more than 99.7%. Albite in K-feldspar is also very pure.

Feldspars display intergrowth of albite and potassium feldspar to give perthitic texture or in more blocky isolated patches developed along cleavages or possibly along fractures (Plate V-2 and 3). These textures are particularly evident in K-feldspar albite intergrowths, but albitization of feldspar grains was absent in the samples characterized with early carbonate rich cement (Plate: I-6).

Re-crystallization and Replacement

Re-crystallization has been recorded in the studied samples, however, some coarse crystalline carbonate were produced from re-crystallization of an original finer grained; this may result occupation of the available pore space or partial replacement of the altered grains and cements. Carbonate cements and quartz replaced by pyrite, matrix and pore space replaced by calcite, microfossil replaced by ferroan dolomite (Plate II-4) and replacement of potassic feldspar rims by re-crystallized ferroan dolomite is shown in Plate V-4.

Porosities

Primary Porosity

Primary porosity has been subjected to a range of diagenetic processes resulted complete pore space plugging by authigenic silica cement in interlocking texture as shown in Plate V-5, or by pore filling cements, in which the framework grains floating in early poikilotopic calcite cement (Plate I-6). Partial porosity reduction is indicated by precipitation of authigenic anhydrite, quartz and feldspar overgrowths associated with free pore space (Plate V-6).

Secondary Porosity

Secondary porosity is the effective porosity in the studied samples. It was produced by alteration and dissolution or leaching of unstable minerals such as
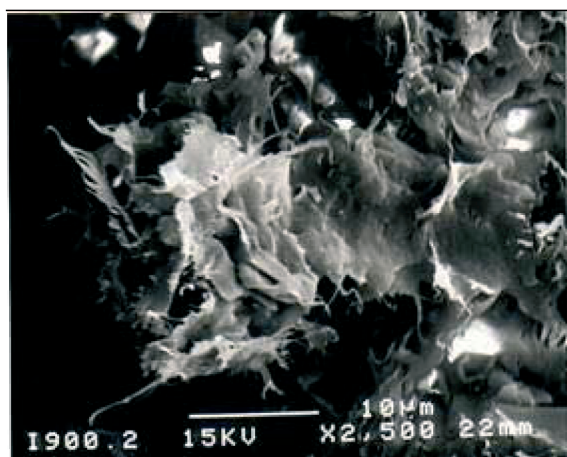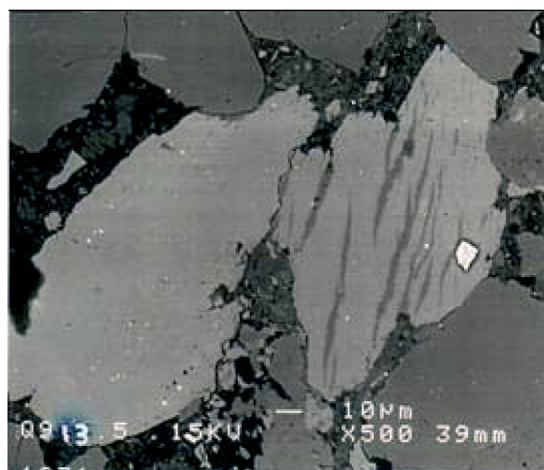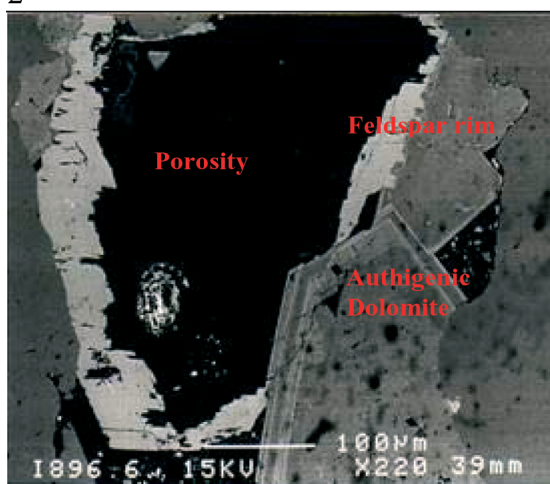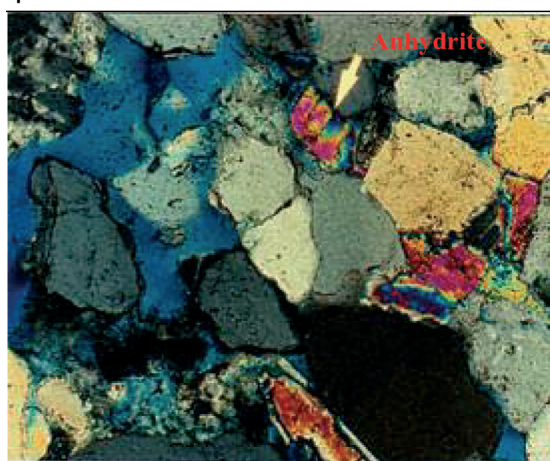
Plate V

Plate V-1   Authigenic illite. II1-32, 49002 (-37392), 512 BT. SEM.
Plate V-2   Perthitic k-feldspar formed from growth of sodium feldspar, probably along fractures. Q1-32, 38132 (-37622), 172 BT. BSE.
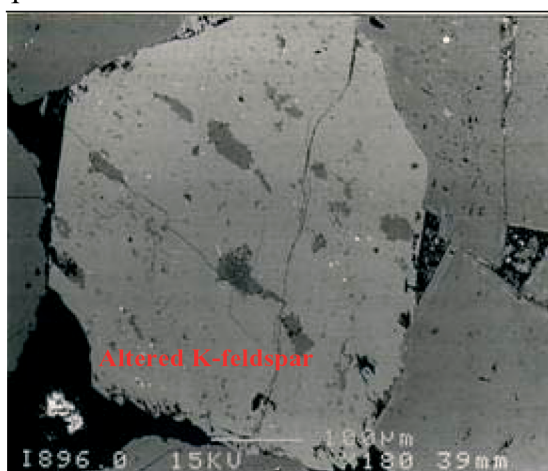*Plate* V-3   K-feldspar with patchy albite intergrowth in weakly orientated zones along cleavage. Note later kaolinization of albite (darker zones). II1-32 48962 (-36352), 472 BT. BSE.
Plate V-4   Late authigenic dolomite crystals replacing the margins of k-feldspar rims, and precipitating in secondary porosity produced from dissolution or alteration of feldspar grain. II1-32, 48962 (-37372), 472 BT. BSE.
Plate V-5   Quartz overgrowth and authigenic kaolin filling the pore space. FF-32, 4651' (-3746').23' BT. BSE.
Plate V-6   Quartz and feldspar overgrowths, anhydrite and clay minerals are partially reducing the secondary porosity. II1-32, 49082 (37472), 592 BT. BSE.
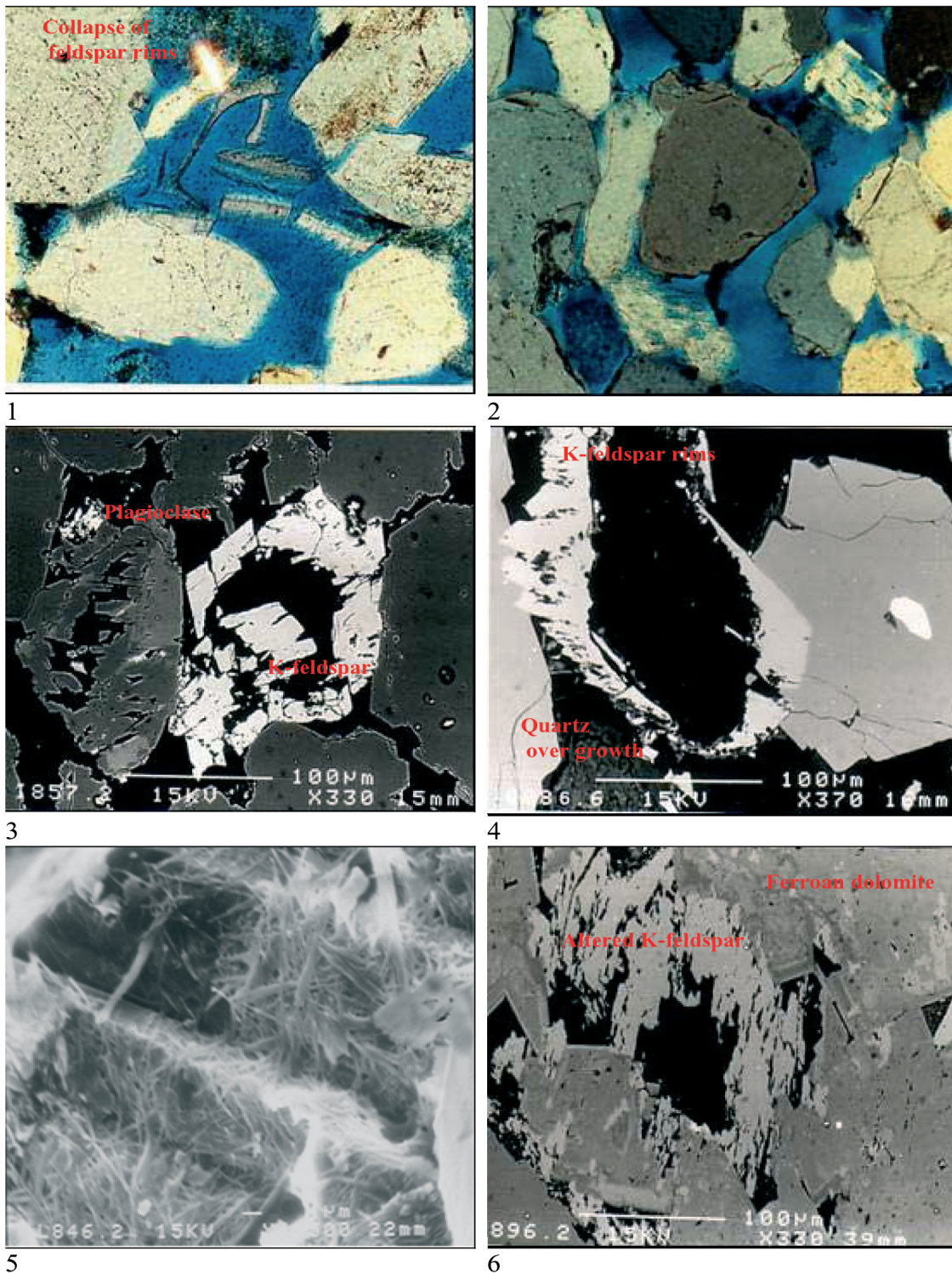
Plate VI

Plate VI-1   Oversized intergranular porosity produced due to alteration of the whole detrital feldspar grain and collapse of the overgrowth rim. MM1-32, 47372 (-39802), 12.52 , BT. TS. XP x20.

Plate VI-2   Secondary porosity in elongation form due to dissolution of cement matrix and unstable grains. LL1-32, 48642 .4 (-37542 .4), 292 BT. TS. XP x10.

Plate VI-3   Secondary porosity formed from alteration of detrital feldspar grains. Showing that the albite overgrowth precedes k-feldspar overgrowth. II1-32, 48572 (-36962),82 BT. BSE.

Plate VI-4   Early or cotemporary development of feldspar overgrowth relative to quartz overgrowth. LL1-32, 4856' (-3746'), 21' BT. BSE.

Plate VI-5   Late development of illite forming after development of quartz overgrowth.   LL1-32, 4846' (-3736'), 11' BFT. SEM.

Plate VI-6   Development of large ferroan dolomite crystals replacing altered k- feldspar grain. II-32, 4896', (-3735'), 47.BT. BSE.

feldspars, mica and cement, displaying oversized and elongated pores (Plate VI-1 and 2). Minor secondary porosity, such as partial dissolution with corrosion of quartz and feldspar grains, open grain fractures indicated in Plate I-2. These porosities matched the classification by Schmidt and McDonald (1979).

The average porosity as calculated from point counting ranges between, 7 % to 19% of total rock volume with an average of 10%, in the wells JJ1, Q1, LL1, II1, FF1, and MM1-32. Clay and carbonate rich levels display very low porosity ranging between 2 to 6.7% of total rock volume, whereas dense dolomite thin beds show zero porosity.

Major Upper Bahi Formation Porosities

1-Intergranular and intercrystalline porosities are the most common porosities in the formation, ranging between 65 and 80% of the total porosities, particularly in the clean sandstone sequences, which are characterized by high porosity (Plate. VI-2).

2- Grains and crystals alteration and dissolution porosities are the second most important porosity in the formation. It is produced from alteration and dissolution of plagioclase feldspar such as albite, alkali feldspar (Plate VI-3), or from corrosion of some quartz grains and alteration or dissolution of some accessory minerals and carbonate crystals. These porosities types are estimated to vary form 5% in the well-cemented levels to 15 % of total in clean sandstone levels.

3- Cement and matrix dissolution porosity represented by very low percentage, present in the well-cemented and fine grained sequences, and is relatively high in the coarse and highly porous sequences (Plate. VI-1).

Relative Timing and Sequence of Diagenetic Processes in the Upper Bahi Formation

Inter-relationships between the various diagentic features of the sandstone samples show that this part has a complex paragenesis. The relative order of events, broadly classified under early and late stages is summarized in Table 2.

Table 2. Summary of the suggested paradiagenetic sequences of the Upper Bahi Formation.

Temperature	0^0 C	70^0 C	$+100^0$C
Depth	Surface	2 km	3 km
Minerals/Events	Eodiagenetic		Mesodiagenetic
Bioturbation	==		
Glauconite	====—-		
Iron oxides	====—		
Calcite	========		
Dolomite	====——-		=====———
Ferroan dolomite		===	=======
Kaolin	======———		=====———
Illite		===	=======———
Chlorite		===	===
Pyrite	=====—-		====——
Mechanical compaction		=======	=====———
Chemical compaction		====	==============————
Mica deformation		===	=======——-
Fossil replacement	====—		========——
Grain dissolution / alteration		====	========—————-
Feldspar albitization		===	========—————-
Feldspar kaolinization		=	==========————-
Mica nucleation of kaolin		=	========———
Albite overgrowth		=	==========———
K-feldspar overgrowth		==	============——
Grain fractures		===	========———
Quartz overgrowth		==	============————
Anhydrite		=-	=======——
Feldspar rims replacement			===——-
Collapse of overgrowth rims			==—-

Early Diagenetic Features (Eodiagenesis)

Bioturbation, and precipitation of glauconite, pyrite and carbonate cement are the most common early events indicated in the marine sequences which represent the uppermost part of the Bahi Formation, whereas, kaolin, haematite and silica – chalcedony were precipitated in the fluvial sequences. Following Morad (2004), eodiagensis is though to have taken place at shallower depths ranging from surface up to 2km, with temperature ranges from surface temperature up to 70°C (Table 2).

Late Diagenetic Features - Burial (Mesodiagenesis)

Quartz and Feldspar Overgrowths and Feldspar Albitization: The next important development was the first of two episodes of quartz overgrowth. This was probably related to pressure solution/ re-precipitation, although some could have been precipitated from formation waters flowing through the system. This phase of quartz overgrowth may be contemporary or preceded development of K-feldspar overgrowths (Plate. VI-4). The mesodiagenesis possibly occurred after the sediment had been buried to depth of 2km or more and at subsurface temperature ranging from 70° C up to about 100° C (Morad, 2004).

The relationship of the quartz overgrowths to albite overgrowth and albitization is less easy to establish. Lack of albitization of K-feldspar overgrowths on albitized K-feldspar grains suggests that albitization of the parent grains preceded the overgrowth. The distinction is less clear in albite overgrowths on albitized plagioclase where it is often difficult to distinguish overgrowth from albitized parts of the grains. It can be seen, however, that K-feldspar overgrowth is later than albite overgrowth (Plate.VI-3).

Major Phase of Dissolution and Porosities Forming: The major development of secondary porosity at this stage can be related to a change in the composition of the formation waters to more acidic forms. It is possible that acidic formation waters arose from CO_2-rich waters related to maturation of kerogens or from water expelled from compacted shale, where the CO_2 was generated from biotic decarboxylation reactions.

Development of secondary porosity brought about by dissolution of plagioclase feldspars to give skeletal forms, further rims alteration may caused overgrowth collapse (VI-1 and 2).

Major Development of Clay Minerals: Early kaolin crystals engulfed by quartz overgrowth (Plate IV-5), and entrapment of kaolin crystals by feldspar overgrowth has been observed in Plate IV-6. That kaolin is produced from alteration of feldspar grains and may represent late diagenesis phase. The age relationship of the expanding micas to quartz overgrowth is shown in Plate IV-4, where the kaolin expands into the pore space and between the grains with presence of quartz overgrowth indicating that the kaolin is formed later. In addition, albite patches within some albitized grains are also altered to kaolin suggested later forming (Plate V-2 and 3). Illite in some samples also appears to be produced later than quartz overgrowth as seen in Plate VI-5.

Replacement and Re-Crystallization Phase: Replacement of some framework grains by re-crystallized carbonates, pyrite and anhydrite appears to be the final phase leading to the observed composition and porosity. This event is represented by precipitation of anhydrite and ferroan dolomite in the pore space replacing the altered feldspar grains (Plate II-6 and V-4).

Replacement of some framework grains by pyrite appears to be the final phase leading to the observed composition and porosity.

Timing of Carbonate Precipitation: There are at least two phases of calcite precipitation in the upper Bahi Formation. The first phase is demonstrably before a phase of quartz overgrowth (Plate I-6), while phase two, was formed later than precipitation of the quartz overgrowth (Plate II-1). Early dolomite is represented in thin lamina (Plate II-2). Ferroan dolomite indicates that formed later than several diagenetic events such as development of the overgrowths and alteration of feldspars (Plate VI-6).

Timing of Mica Deformation: It is clear that deformation of mica occurred before development of a phase of dissolution secondary porosity and probably before the first phase of the overgrowths. It would thus correspond to early eodiagenetic compaction phase (Plate (I-3).

CONCLUSION

The upper Bahi Formation had been subjected to strong and complex diagenesis process, in which the unstable minerals are physically exposed to compaction, deformation and fracturing of the grains, and chemically suffered alteration, dissolution, etching, precipitations and replacement. The diagenesis processes are divided into early and late diagenesis: Early diagenesis or *eodiagenesis stage* physical and the chemical changes took place sooner after deposition; these included primary compaction of the grains, precipitation of the carbonate cement and forming clay minerals such as kaolin. Late diagenesis or burial (*mesodiagenetic stage*), in which most of the physical and chemical changes occurred, such as precipitation of quartz and feldspars overgrowths, authigenic clay minerals and precipitation of late carbonate and anhydrite cements. The diagenetic processes strongly affected the reservoir quality such as porosity and changed the framework composition. Timings and possible phases of the paradiagenetic sequence are summarized in Table 2.

Further work that would help refine age relationships would be fluid inclusion studies to establish temperatures and hence times of formation of the overgrowths. Isotopic study is recommended to determine the Bahi Formation age.

ACKNOWLEDGEMENTS

REFRENCES

Ahmid, M., 2003. Petrography of the uppermost Bahi Formation in the west Az-Zahrah (B) Field, Az-Zahrah - Al-Hufrah Platform, NW Sirt Basin, Libya. *Petroleum Res. J.*, **15**, 33-48.

Baird, D. W., 1964. *Stratigraphy of the Bahi Sandstone, Sirte Basin, Libya*. (Internal Report no. 54), Oasis Oil Company - Libya Inc.

Barr, F. T. and Weegar, A. A., 1972. Stratigraphic nomenclature of the Sirte Basin, Libya. *The Petrol. Explor. Soc. Libya, Tripoli*. 179 p.

Kastner, M. and Siever, R. 1979. Origin of authigenic feldspar in carbonate rocks. *Geol. Soc. Am., Spec. paper*, no. **121**, 155-156.

Khalifa, M. A., 1997. Provenance and diagenesis of the upper Bahi Sandstone- Cretaceous-in the northwest Dahra oilfield, Sirt Basin, Libya. M. Phil thesis, Earth Sciences Department. Manchester University, 284 p.

Morad, S., 2004. Diagenesis and reservoir quality evolution of sandstones. Seminar at PRC, Libya.

Saigal, G. C., Morad, S., Bjorlkke, K., Egeberg, P. K., and Aagaared, P., 1988. Diagenetic albtization of detrital K-feldspar in Jurassic, Lower Cretaceous and Tertiary clastic reservoir rocks, from offshore Norway I. textures and origin. *J. Sediment. Petrology*, **58**, no.6. 1003-1013.

Schmidt, V., and McDonald, D. A., 1979. The role of the secondary porosity in the course of sandstone diagenesis. *Soc. Econ. Palaeontol. Mineral.*, no. 26, 175-207.

Sghair, A. M., 1996. Petrography, diagenesis and provenance of the Bahi Formation in the western part of the Sirt Basin, Libya. In: Salem M. J., Al Hawat A. S., and Sbeta A. M. (eds.) *The Geol. Sirt Basin*, First Symposium of the Sedimentary Basins of Libya, Held at Tripoli, October 10-13-1993. Elsevier, Amsterdam. **II**, 65-81.

Walker, T. R., 1984. Diagenetic albitization of potassium feldspar in arkosic sandstone. *J. Sediment. Petrology*, **54**, no. 1, 3-16.

Wilson, J., 1987. X-Ray powder diffraction methods. In: Wilson, M. J., (ed.) *A Hand Book of Determinative Methods in Clay Mineralogy*, Blackie-Chapman and Hall, New York, 26-98 p.